Article

Ferrocenylundecanethiol Self-Assembled Monolayer Charging Correlates with Negative Differential Resistance Measured by Conducting Probe Atomic Force Microscopy

Alexei V. Tivanski, and Gilbert C. Walker

J. Am. Chem. Soc., **2005**, 127 (20), 7647-7653• DOI: 10.1021/ja0514491 • Publication Date (Web): 03 May 2005

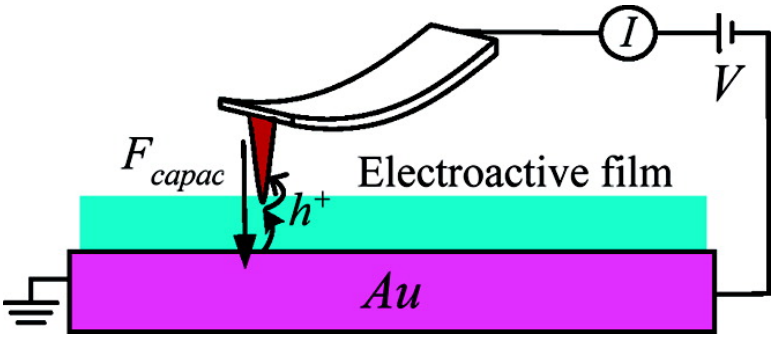

More About This Article

Additional resources and features associated with this article are available within the HTML version:

- Supporting Information
- Links to the 12 articles that cite this article, as of the time of this article download
- Access to high resolution figures
- Links to articles and content related to this article
- Copyright permission to reproduce figures and/or text from this article

View the Full Text HTML

J|A|C|S
ARTICLES
Published on Web 05/03/2005

Ferrocenylundecanethiol Self-Assembled Monolayer Charging Correlates with Negative Differential Resistance Measured by Conducting Probe Atomic Force Microscopy

Alexei V. Tivanski† and Gilbert C. Walker*,‡

Contribution from the Department of Chemistry, University of Pittsburgh, Pittsburgh, Pennsylvania 15260, and Department of Chemistry, University of Toronto, Toronto, Ontario, M5S 3H6, Canada

Received March 7, 2005; E-mail: gilbert.walker@utoronto.ca

Abstract: Electrical and mechanical properties of metal−molecule−metal junctions formed between Au-supported self-assembled monolayers (SAMs) of electroactive 11-ferrocenylundecanethiol ($FcC_{11}SH$) and a Pt-coated atomic force microscope (AFM) tip have been measured using a conducting probe (CP) AFM in insulating alkane solution. Simultaneous and independent measurements of currents and bias-dependent adhesion forces under different applied tip biases between the conductive AFM probe and the $FcC_{11}SH$ SAMs revealed reversible peak-shaped current−voltage ($I-V$) characteristics and correlated maxima in the potential-dependent adhesion force. Trapped positive charges in the molecular junction correlate with high conduction in a feature showing negative differential resistance. Similar measurements on an electropassive 1-octanethiol SAM did not show any peaks in either adhesion force or $I-V$ curves. A mechanism involving two-step resonant hole transfer through the occupied molecular orbitals (MOs) of ferrocene end groups via sequential oxidation and subsequent reduction, where a hole is trapped by the phonon relaxation, is proposed to explain the observed current−force correlation. These results suggest a new approach to probe charge-transfer involving electroactive groups on the nanoscale by measuring the adhesion forces as a function of applied bias in an electrolyte-free environment.

Introduction

Negative differential resistance (NDR), that is, a negative slope in the current−voltage ($I-V$) curve, has been observed for resonant tunneling charge transfer through metal−molecule−metal (m−M−m) junctions.[1−7] In these junctions, a molecular film is typically sandwiched between two metal electrodes. Tunnel contact barriers and the weak coupling between the electronic states of the molecules and the metal electrodes indicate that charges trapped on the molecules can play a significant role in NDR,[8] but direct experimental measurement of the extent of charge trapping has been limited.[6,7]

The scanning probe microscope, where the probe serves as one of the metal electrodes in scanning tunneling microscopy (STM)[1−4] and conducting probe atomic force microscopy (CP-AFM),[5−7,9−18] has been commonly used to form and study the electrical and structural properties of m−M−m junctions. The electronic properties of a junction are sensitive to the effects of deformation caused by the interaction force between the probe and the sample;[10−15] thus, it is valuable to measure force and current simultaneously to properly characterize charge transfer through molecular junctions. This can be achieved directly using CP-AFM, unlike STM where the contact force is neither known nor controlled. The capability of AFM to measure precisely the contact forces between the probe and the sample surface allows independent and simultaneous measurement of the current and the contact force between the probe and the sample. CP-AFM also presents the opportunity to measure directly the electrical capacitance at an interface and hence trapped charges.

† University of Pittsburgh.
‡ University of Toronto.

(1) Gorman, C. B.; Carroll, R. L.; Fuierer, R. R. *Langmuir* **2001**, *17*, 6923.
(2) Wassel, R. A.; Credo, G. M.; Fuierer, R. R.; Feldheim, D. L.; Gorman, C. B. *J. Am. Chem. Soc.* **2004**, *126*, 295.
(3) Tao, N. J. *Phys. Rev. Lett.* **1996**, *76*, 4066.
(4) Han, W.; Durantini, E. N.; Moore, T. A.; Moore, A. L.; Gust, D.; Rez, P.; Leatherman, G.; Seely, G. R.; Tao, N.; Lindsay, S. M. *J. Phys. Chem. B* **1997**, *101*, 10719.
(5) Rawlett, A. M.; Hopson, T. J.; Nagahara, L. A.; Tsui, R. K.; Ramachandran, G. K.; Lindsay, S. M. *Appl. Phys. Lett.* **2002**, *81*, 3043.
(6) Fan, F. F.; Yang, J.; Cai, L.; Price, D. W., Jr.; Dirk, S. M.; Kosynkin, D. V.; Yao, Y.; Rawlett, A. M.; Tour, J. M.; Bard, A. J. *J. Am. Chem. Soc.* **2002**, *124*, 5550.
(7) Fan, F. F.; Yao, Y.; Cai, L.; Cheng, L.; Tour, J. M.; Bard, A. J. *J. Am. Chem. Soc.* **2004**, *126*, 4035.
(8) Kuznetsov, A. M.; Sommer-Larsen, P.; Ulstrup, J. *Surf. Sci.* **1992**, *275*, 52.
(9) Cui, D.; Zarate, X.; Tomfohr, J.; Sankey, O. F.; Primak, A.; Moore, A. L.; Moore, T. A.; Gust, D.; Harris, G.; Lindsay, S. M. *Nanotechnology* **2002,** *13*, 5.
(10) Gomar-Nadal, E.; Ramachandran, G. K.; Chen, F.; Burgin, T.; Rovira, C.; Amabilino, D. B.; Lindsay, S. M. *J. Phys. Chem. B* **2004**, *108*, 7213.
(11) Leatherman, G.; Durantini, E. N.; Gust, D.; Moore, T. A.; Moore, A. L.; Stone, S.; Zhou, Z.; Rez, P.; Liu, Y. Z.; Lindsay, S. M. *J. Phys. Chem. B* **1999**, *103*, 4006.
(12) Wold, D. J.; Frisbie, C. D. *J. Am. Chem. Soc.* **2001**, *123*, 5549.
(13) Lee, T.; Wang, W.; Klemic, J. F.; Zhang, J. J.; Su, J.; Reed, M. A. *J. Phys. Chem. B* **2004**, *108*, 8742.
(14) Tivanski, A. V.; Bemis, J. E.; Akhremitchev, B. B.; Liu, H.; Walker, G. C. *Langmuir* **2003**, *19*, 1929.
(15) Tivanski, A. V.; He, Y.; Borguet, E.; Liu, H.; Walker, G. C.; Waldeck, D. H. *J. Phys. Chem. B* **2005**, *109*, 5398.
(16) Ishida, T.; Mizatani, W.; Aya, Y.; Ogiso, H.; Sasaki, S.; Tokumoto, H. *J. Phys. Chem. B* **2002**, *106*, 5886.
(17) Suganuma, Y.; Trudeau, P.-E.; Dhirani, A.-A. *Phys. Rev. B* **2002**, *66*, 241405.
(18) Tivanski, A. V.; Walker, G. C. *Langmuir*, submitted for publication.

Scheme 1. General Schematic of the CP-AFM Experiment Used in This Study

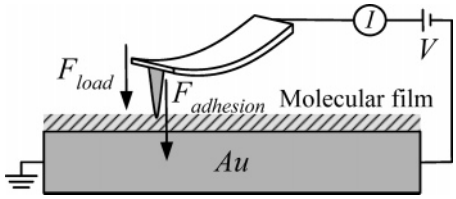

Recently, we studied electroactive polythiophene monolayers self-assembled on a gold surface.[14] By measuring the "pull-off" forces under different biases, we observed a peak in the dependence of the adhesion force as a function of bias that apparently originated from an oxidation state change of the polymer chains under the negatively charged AFM tip. Here, we report electrical conduction measurements of electroactive m−M−m junctions formed between Au-supported self-assembled monolayers (SAMs) of 11-ferrocenylundecanethiol ($FcC_{11}SH$) and a Pt-coated AFM tip using CP-AFM in bicyclohexyl solvent. The objective is to correlate the measured currents and the bias-dependent adhesion force under different applied biases between the conductive AFM probe and the molecular film. Ferrocenylundecanethiol was chosen for several reasons. First, recent STM measurements demonstrated that similar molecules displayed NDR in STM tip/SAM/Au junctions.[1,2] In addition, $FcC_{11}SH$ molecules can be easily and reversibly oxidized under relatively small applied biases due to the presence of strong electron-donating, ferrocene end groups, and oxidation was expected to play a significant role in NDR. We explored the extent of charge trapping within the electroactive m−M−m junctions when negative differential resistance was observed. Additionally, electric force measurements along with theoretical modeling both in and out of contact with a nonelectroactive 1-octanethiol (C_8SH) SAM were also performed.

Experimental Section

SAM Preparation. All self-assembled monolayers were formed by exposing the freshly prepared Au(111) facet of a single crystalline bead[19] to 1 mM 1-octanethiol (C_8SH, Sigma-Aldrich Corp., St. Louis, MO) or 5 mM 11-ferrocenylundecanethiol ($FcC_{11}SH$, Dojindo Molecular Technologies, Inc., Gaithersburg, MD) solutions in purified (by distillation) tetrahydrofuran (THF) with soaking times between 4 and 24 h. After assembly, samples were thoroughly rinsed in purified THF and dried in a stream of nitrogen gas. All preparations were performed at room temperature, and all samples were used within 1 day of preparation.

Conducting Probe AFM Measurements. The CP-AFM measurements (see Scheme 1) were performed using a commercial contact mode AFM (Molecular Force Probe, Asylum Research, Santa Barbara, CA) modified in Pittsburgh for conducting probe experiments. Different fixed tip biases were applied, and currents through the junctions were measured (using a picoammeter, Chem-Clamp, Dagan Corp., Minneapolis, MN) as a function of vertical piezo displacement, simultaneously with independent force detection between the tip and the sample. The sample was not scanned in horizontal directions; rather, the AFM tip was allowed to thermally drift over the sample surface. Measured "pull-off" forces and currents for different contact forces over different surface locations were averaged over the number of repeated measurements to obtain averaged bias-dependent adhesion forces and force-dependent current−voltage ($I-V$) characteristics of the junction. The $I-V$ and $F-V$ profiles were obtained by stepping the voltage in 0.05-V increments, with approximately 5-s delays between successive I or F measurements. The experimental error is dominated primarily by the uncertainty in the exact number of molecules forming the junction. Because the tip drifts over the surface, variations in the number of contacting molecules may cause fluctuations in the measured current and the adhesion force. In addition, variations in the chemical environment across the SAM surface could also introduce experimental error in both force and current measurements.

All experiments reported here were performed in an insulating bicyclohexyl solvent (99.0%, Fluka, Switzerland) to reduce water contamination and decrease the adhesion forces between the probe and the sample. Au- and Pt-coated V-shape silicon cantilevers (MikroMash, Estonia) were used, with force constants that ranged from 0.3 to 0.5 N/m and tip radii of curvature of less than 25 nm. Cantilevers were cleaned in piranha solution (1:3 of 30% H_2O_2/98% H_2SO_4) for 5 min, rinsed in ultrapure water (>18 MΩ·cm) for 1 min, then soaked in hydrofluoric acid for 20 s, and finally rinsed again in ultrapure water for 1 min followed by drying under vacuum. *Caution! Piranha solution is a very strong oxidant and is extremely dangerous to work with; gloves, goggles, and a face shield should be worn.*

To decrease the probable effect of tip damaging over repeated measurements, when the conduction between the tip and sample was observed to decrease under similar conditions or evolution of the force curves over repeated measurements was observed, we stopped collecting data and changed the tip. Forces higher than 30 nN were not applied due to the noticeably quick decrease in the magnitude of observed currents indicating apparent damage of the conductive coating on the tip. Depending on the coating of the tip, typically 100−500 force plots were collected with the same tip. All measurements were carried out at room temperature.

Results and Discussion

(A) Bias-Dependent Force Measurements on 1-Octanethiol SAMs and Models. We first describe electric force measurements and theoretical models of a tip both in and out of contact with a nonelectroactive 1-octanethiol (C_8SH) SAM. If a voltage is applied between two different conducting materials (in this case a conducting AFM tip and a conducting substrate), then an attractive electrostatic force due to the tip−sample capacitance[11,14,20] is added to the other forces experienced by the AFM probe. For the typical probe geometry, the total capacitance can be approximated as a sum of the contributions due to the tip apex, tip body, and the cantilever. The electrostatic force between the conductive cantilever body and the conductive sample system can be approximated by a parallel plate capacitor,[21] and in our case it is several piconewtons and has a very weak tip−sample separation dependence. Since the electrostatic forces observed here are much larger, we will neglect the electrostatic force acting on the cantilever body. The tip body resembles an inverted pyramid with a rounded tip. At very small tip−sample separations ($z < R$, where R is the tip radius of curvature and z is the tip−sample separation), the spherical tip apex provides the major contribution to the force, and an analytical expression can be obtained from the conductive sphere and a semi-infinite conductive plane model[22] while for larger tip−sample separations ($z > R$), a uniformly charged line model[23] can provide the closest description. By combining these

(19) Clavilier, J. F.; Guinet, G.; Durand, R. *J. Electroanal. Chem.* **1980**, *107*, 205.
(20) Cui, X. D.; Zarate, X.; Tomfohr, J.; Primak, A.; Moore, A. L.; Moore, T. A.; Gust, D.; Harris, G.; Sankey, O. F.; Lindsay, S. M. *Ultramicroscopy* **2002**, *92*, 67.
(21) Martin, Y.; Abraham, D. W.; Wrickramasinghe, H. K. *Appl. Phys. Lett.* **1988**, *52*, 1103.
(22) Terris, B. D.; Stern, J. E.; Rugar, D.; Mamin, H. J. *Phys. Rev. Lett.* **1989**, *63*, 2669.

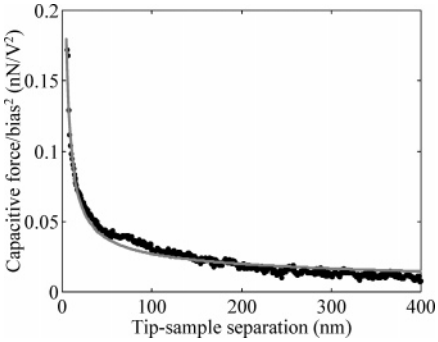

Figure 1. Averaged capacitive force (●) between a Au-coated tip and a C_8SH monolayer normalized by the square of tip bias is shown as a function of tip−sample separation. The solid gray line represents the best fit using the analytical expression in eq 1.

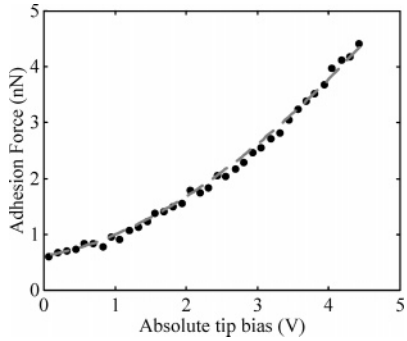

Figure 2. Experimental (●) and theoretical (gray dashed line) bias-dependent adhesion force between the Au-coated probe and the C_8SH SAM in bicyclohexyl solvent is shown as a function of absolute tip bias.

contributions, the total capacitive force (F_{capac}) for a realistic tip shape including tip body and spherical tip apex can be approximated as

$$F_{capac} = \pi\epsilon_0 V^2\left[\frac{R}{z} + \frac{4}{\alpha^2}\ln\left(\frac{H}{4z}\right)\right] \quad (1)$$

where V is the difference in potential between the probe and the sample, H is the total tip length, $\alpha = \ln[(1 + \cos\theta)/(1 - \cos\theta)]$, and θ is the half angle of the tip body. It is important to point out that even in the absence of an applied potential, a capacitance force may still exist due to the contact potential difference between different materials.[24]

The presence of a thin organic layer of high dielectric constant grafted on the conductive substrate should not strongly modify the capacitive forces assuming that the electrostatic field in the dielectric material is much weaker than that in the solution space between the conductive probe and the conductive surface. Thus, to take into account the organic film, it suffices to replace tip−sample separation (z) in eq 1 by an effective distance $z + d/\epsilon_r$, where d and ϵ_r are the thickness and the dielectric constant of the organic film, respectively. With respect to the experimental force plots, the tip−sample separation measured by AFM is between the probe and the organic film, yet the relevant tip−sample separation in the capacitive forces is between the probe and the substrate on which the molecular film is grafted.

Equation 1 suggests that noncontact attractive capacitive forces have a parabolic dependence upon the applied tip bias. For the Au-coated AFM probe over a C_8SH SAM in bicyclohexyl solvent, all force dependencies were overlapped very closely after normalizing all experimental noncontact capacitive forces with square applied biases, confirming the parabolic bias dependence. The averaged normalized noncontact capacitive force (•) as a function of tip−sample separation is shown in Figure 1. The zero force was selected as the force when the tip was far away (∼500 nm) from the surface.

From eq 1, an analytical expression for the capacitive noncontact attractive force can be compared with the experimental results. Since the real dimensions for the Au-coated AFM tip used in these experiments are not known precisely, a total length, half angle, and apex radius were used as free fit parameters. The solid gray line in Figure 1 shows the best fit by the model of the noncontact capacitive force as a function of the tip−sample separation. The fit indicates a half angle $\theta = 10.3 \pm 0.2°$, a tip radius of curvature $R = 27 \pm 0.4$ nm, and a total length of the tip $H = 22 \pm 2$ μm, which are all close to the manufacturer's reported values (15°, <40 nm, and 20 μm, respectively). The thickness of the C_8SH SAM was estimated as 1.04 nm from molecular length, as obtained from semiempirical calculations using the PM3 method, and a relative dielectric constant was taken to be 2. Reasonably good agreement between the theoretical and experimental results suggests that the long-range noncontact attractive forces acting on the conductive probe over a C_8SH SAM can be described using the analytical expression in eq 1.

Using our definition of the adhesion force as the "pull-off" force relative to the zero force when the tip is far away from the surface, we can plot the experimentally measured, bias-dependent adhesion force between the Au-coated AFM probe and the C_8SH monolayer as a function of the applied tip bias. Bias-dependent adhesion forces were obtained by averaging over more than 1000 repeated measurements of "pull-off" forces under different tip biases, with the tip contacting different surface spots of the SAM. Due to the fact that the bias-dependent adhesion forces in this case were fully symmetric for both tip bias polarities, the experimentally obtained adhesion force is shown in Figure 2 (•) as a function of the absolute tip bias. Each data point shown in Figure 2 represents the mean value of bias-dependent adhesion force for a series of ∼30 repeated measurements under a particular bias; the standard deviation of the mean is typically smaller than the size of the printed point.

To calculate the bias-dependent adhesion force between the conductive probe and the sample, the bias-dependent tip−sample separation (z_{off}) at which the tip jumps away from the surface must be estimated. This event occurs when the gradient of interaction force becomes less or equal to the spring constant of the cantilever. This distance can be determined from the following equation:

$$-\frac{dF_{capac}(z,V)}{dz} = k_c \quad (2)$$

where k_c is the spring constant of the cantilever. By substituting eq 1 into eq 2, one obtains eq 3, which is an analytical expression for the bias-dependent tip−sample separation at which the tip jumps away from the surface.

$$z_{off} = d/\epsilon_r + |V|\sqrt{\pi\epsilon_0 R/k_c} \quad (3)$$

(23) Hao, H. W.; Baro, A. M.; Saenz, J. *J. Vac. Sci. Technol., B* **1991**, *9*, 1323.
(24) Hudlet, S.; Saint Jean, M.; Guthmann, C.; Berger, J. *Eur. Phys. J. B* **1998**, *2*, 5.

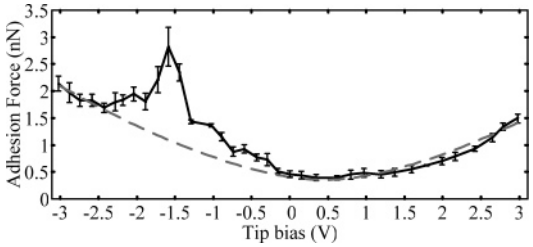

Figure 3. Experimental (points with error bars) and theoretical (dashed gray line) bias dependent adhesion forces between the Pt-coated probe and the $FcC_{11}SH$ SAM in bicyclohexyl solvent, as a function of the applied tip bias. The error bars represents the standard deviation of the mean for a series of ~20 repeated measurements under a particular bias.

Here, the gradient of interaction force due to only the spherical tip apex contribution was considered, since the gradient of force due to the tip body was negligible. By substituting eq 3 back into eq 1, the theoretically predicted dependence of the adhesion force as a function of applied tip bias can be written as:

$$F_{adh}(V) = \pi\epsilon_0 V^2 \left\{ \frac{R}{d/\epsilon_r + |V|\sqrt{\pi\epsilon_0 R/k_c}} + \frac{4}{\alpha^2}\ln\left[\frac{H}{4(d/\epsilon_r + |V|\sqrt{\pi\epsilon_0 R/k_c})}\right]\right\} \quad (4)$$

The first term in eq 4 represents the spherical tip apex contribution, and the second term provides the contribution from the tip body to the bias-dependent adhesion force. The intrinsic adhesion force of 0.62 nN (determined at 0 V applied tip bias) has been added to the calculated dependence. Excellent agreement between the theoretical (gray dashed line in Figure 2) and experimental results suggests that the bias-dependent adhesion forces between the conductive probe and nonelectroactive C_8-SH SAM can be described using the analytical expression in eq 4. This agreement is especially noteworthy since the fitted values of the tip dimensions obtained from the noncontact capacitance model were used to make this theoretical prediction of the adhesion force. No additional fitting was required.

(B) Bias-Dependent Force and Current Measurements on Electroactive 11-Ferrocenylundecanethiol SAMs. Unlike C_8-SH molecules, $FcC_{11}SH$ molecules can be easily and reversibly oxidized under relatively small applied biases due to the presence of strong electron-donating, ferrocene end groups. m−M−m junctions were formed between Au-supported SAMs of electroactive $FcC_{11}SH$ and a Pt-coated AFM tip. As done for C_8SH, experimental measurements and data analyses were made for the noncontact bias-dependent capacitive forces to determine the Pt-coated tip radius of curvature; $R = 11 \pm 0.5$ nm. The contact potential difference between Au and Pt materials was found to be $V_r = 0.45 \pm 0.05$ V, which corresponds well to the difference in the work functions of Au (5.2 V) and polycrystalline Pt (5.65 V). The thickness of the $FcC_{11}SH$ SAM and the relative dielectric constants were taken to be 2.37 nm and 2, respectively.[25] The noncontact capacitive force results were consistent with those obtained for the Au-coated tips over C_8SH monolayers and were well described using our capacitive force model.

In the same way as for C_8SH, experimental measurements and data analyses were performed for the bias-dependent adhesion force. Figure 3 shows the measured adhesion forces (points with error bars as the mean and the standard deviation of a series of ~20 repeated measurements under a particular bias) between the Pt-coated AFM probe and the $FcC_{11}SH$ SAM in bicyclohexyl solvent as a function of applied tip bias. Bias-dependent adhesion forces were obtained by averaging over hundreds of repeated measurements of "pull-off" forces under different tip biases with the tip contacting different surface regions of the SAM. Bias magnitudes higher than 3 V were not applied to avoid high currents passing from the conductive probe to the conductive substrate, which might irreversibly damage the monolayer. The theoretically predicted dependence (dashed gray line) was plotted using eq 4 with fitted parameters obtained from the noncontact capacitive force measurements, and no additional adjustment of the parameters was performed. The intrinsic adhesion force of 0.35 nN has been added to the calculated dependence.

As can be seen in Figure 3, the experimental dependence of the bias-dependent adhesion force in the negative bias region clearly deviates from the theoretical dependence in the bias region between −0.2 and −2.4 V, while the experimental data in the positive tip bias region closely follow calculated dependence. The approximate maximum of the adhesion deviation peak is around -1.6 ± 0.12 V (with a peak width at half-maximum of about 0.5 ± 0.1 V) with a magnitude of 1.7 ± 0.4 nN greater than the theoretical dependence. It is noteworthy that this result is significantly different from measurements on the nonelectroactive C_8SH SAM where the experimental dependence of the adhesion forces closely follows the theoretically calculated dependence for both tip bias polarities. It is important to mention that in our previous measurements on a Au-coated AFM tip/1,4 benzene dimethanethiol SAM/Au substrate junction,[14] which is not expected to undergo redox transitions in this range of applied biases, no deviation from theoretically predicted behavior was observed as well. However, our CP-AFM measurements on electroactive conjugated polythiophene monolayers, sandwiched between two gold electrodes, did produce an apparent peak in addition to the expected theoretical dependence.[14] This indicates that deviation in the bias-dependent adhesion force is observable regardless of the electrode materials (at least for gold and platinum). Since the observed bias-dependent adhesion force deviation over calculated dependence is positive and the terminal ferrocene groups can be easily oxidized to ferricenium cations (Fc^+), we hypothesize that the adhesion force peak in Figure 3 arises from attractive Coulombic interactions between the negatively charged AFM tip and the terminal Fc^+ cations.

To see if there is a correlation between the measured current and the adhesion force in the negative bias region that could help to explain the origin of the observed adhesion force deviation, electrical conduction measurements were performed under different applied negative tip biases. In this way, the current through the junction was measured as a function of tip−sample separation simultaneously with independent detection of the force between the tip and the sample. Force-dependent current−voltage ($I-V$) characteristics of the junction were obtained by averaging over hundreds of repeated measurements under different tip biases with the tip contacting different surface spots of the SAMs.

Figure 4 shows the averaged current (×) of the $FcC_{11}SH$ SAM in bicyclohexyl solvent under a fixed interaction force of

(25) Ohtsuka, T.; Sato, Y.; Uosaki, K. *Langmuir* **1994**, *10*, 3658.

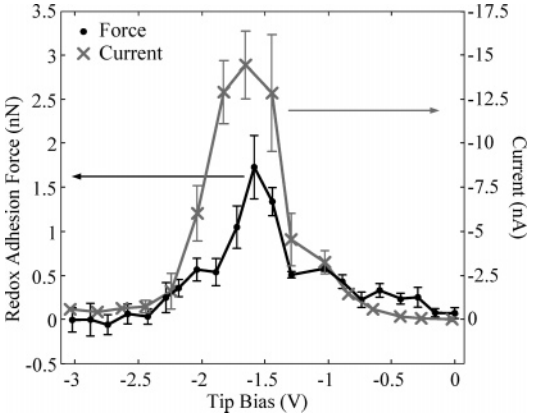

Figure 4. Redox adhesion force (●) and current (×) between the Pt-coated probe and the $FcC_{11}SH$ SAM are shown as a function of the applied tip bias under an interaction force of 5 nN. The error bars represent the standard deviation of the mean.

5 nN; error bars represent the standard deviation of the mean for a series of repeated measurements. The interaction or net force between the tip and underlying film at their contact is considered to be equal to the sum of the loading, intrinsic, and capacitance forces. This interaction force was employed to ensure that a sufficient electrical contact between the conductive probe and the sample is achieved, yet there is no significant monolayer deformation and/or penetration of the tip into the SAM.[18] The averaged peak-shaped $I-V$ characteristic is obtained in the negative tip bias region. No peak-shaped current dependence was observed in the positive bias region between 0 and +3 V where current was increasing monotonically with applied bias (not shown). This is consistent with absence of deviation in the adhesion force dependence for the same positive bias range.

As can be seen in Figure 4, an averaged NDR peak (i.e., a negative slope in the $I-V$ curve) is observed near -1.65 ± 0.18 V (and peak width at half-maximum of 0.6 ± 0.15 V) with a peak-to-valley ratio of 35 ± 8. It is important to mention that Figure 4 was obtained by quasistatic measurements, and not by rapidly sweeping the voltage. The NDR peak position observed here is in excellent agreement with recent STM measurements in dodecane solvent for similar molecules where a peak positioned at -1.6 ± 0.15 V was observed;[1,2] the peak width, however, was approximately four times narrower than that observed here. The reason for this deviation is unclear. However, one possibility may originate from the fact that, unlike STM measurements, in CP-AFM currents are measured with the tip directly contacting the sample. Since the tip drifts over the surface, variations in the number of contacting molecules and in the chemical environment across the SAM surface between measurements could cause fluctuations in the measured current and in the NDR peak position.

The observed $I-V$ characteristics were linear within ± 0.2 V bias range. Figure 5 shows the averaged $I-V$ characteristic in the low-bias range of applied tip biases for the $FcC_{11}SH$ SAM (•) in bicyclohexyl solvent under a fixed interaction force of 5 nN. Ohmic dependences observed in the $I-V$ curves are consistent with the Simmons model in the low-bias region[26,27] for nonresonant tunneling through an m−M−m interface. The linear portion of the $I-V$ curve was fit by a straight line (see Figure 5), and the obtained slope was used to determine the junction resistance. From the fit, the junction resistance for a $FcC_{11}SH$ SAM was 25 ± 2 GΩ.

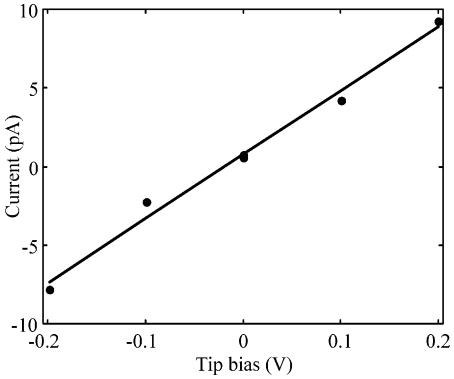

Figure 5. Current (●) between the Pt-coated probe and the $FcC_{11}SH$ SAM and the linear fit is shown as a function of the applied tip bias in the low-bias region under an interaction force of 5 nN.

To compare the measured current and the adhesion force, the calculated adhesion dependence was subtracted from the measured bias-dependent adhesion force, and we thus obtained the deviation force, which we define here as the redox adhesion force. Figure 4 plots the redox adhesion force (•) and the current (×) between the Pt-coated AFM probe over the $FcC_{11}SH$ SAM under the interaction force of 5 nN as a function of applied tip bias. By comparing current and redox adhesion force dependencies shown in Figure 4, it is apparent that, within experimental uncertainty, the biases corresponding to the peak positions in both the bias-dependent adhesion force and the current are the same; also the shape of both curves appears to be similar to the peak width at half-maximum of the redox adhesion force somewhat narrower than that of the current. The correlation between independent measurements of peak-shaped redox adhesion force and current leads us to the conclusion that the mechanisms leading to the observed NDR in current and the peak in the bias-dependent adhesion force should be coupled.

Molecular Orbitals and Peak-Shaped Current and Adhesion Force Dependencies. The relative positions of Fermi energy levels of connecting electrodes and the highest occupied molecular orbital (HOMO) or the lowest unoccupied molecular orbital (LUMO) of the sandwiched molecules is one of the most important factors in understanding charge transport through m−M−m junctions. When the difference between the HOMO (LUMO) and the mean Fermi energy of metal electrodes is large, charge transport through an m−M−m interface under relatively small applied biases is expected to be coherent nonresonant tunneling. In the case of large applied biases, the Fermi energy level can approach the energy of molecular orbitals (MOs) and resonant transition through or in molecular electronic states may take place. For the C_8SH SAM, the molecular HOMO−LUMO gap is quite large (~8 eV), which implies that the charge transfer under relatively small applied biases is primarily dominated by the above mechanism, while under higher biases, electrical breakdown of the molecular film would most likely occur before reaching the energy of MOs. Unlike C_8SH molecules, terminal ferrocene (Fc) groups of $FcC_{11}SH$ have redox-accessible states that lie within 1 eV of the mean Fermi level of metal electrodes,

(26) Simmons, J. H. *Appl. Phys.* **1963**, *281*, 1793.

(27) Sze, S. M. *Physics of Semiconductor Devices*; Wiley & Sons: New York, 1981.

implying that molecular states can be probed under relatively small applied biases without causing electrical breakdown of the film. The exact energies of these electronic states relative to the mean Fermi level of metal electrodes are not straightforward to estimate in a solid environment and in the absence of potential control and a supporting electrolyte, and therefore we are hesitant to provide a more quantitative analysis without further experiments and theoretical computations.

The present m−M−m junction architecture can be considered as localized discrete electronic levels of electroactive Fc groups that are weakly coupled to both metal electrodes and separated from them by two thin insulating metal/molecule junction barriers: the alkylthiolate-S interface[28] on the substrate end and the Pt-coated AFM tip/SAM interface[9] on the other end. The overall tunnel junction is noticeably asymmetrical due to the difference between the metal/electrode contacts: strong chemical bonding S−Au contacts on the substrate side and weak nonbonded (mechanical) AFM tip/ferrocenes contacts on the other side of the molecules.[9] This implies that most of the voltage drop occurs at the AFM tip/molecules interface, and under this consideration, the application of voltage would generally move the Fermi energy of the tip relative to the molecular levels more than those levels shift with respect to the Fermi energy of supporting Au substrate. Similar descriptions have been presented before for both STM and AFM measurements of redox-active moieties.[6,7,29] In this approximation, additional current is expected for the region of applied biases where narrow features in the local density of states (LDOS) of the tip apex couples with the electronic levels of ferrocenes.[30] As larger bias magnitudes are applied, coupling between the tip and the Fc electronic levels decreases, leading to a decrease in the observed current magnitude. Hence, an NDR peak in $I-V$ curve is expected with the peak width primarily determined by the extent of localization in the LDOS of the tip apex. We note that the exact LDOS of the tip apex is expected to change with repeated contact of the tip with the surface. Considering the difference in molecule and electrode contacts employed here and the fact that calculated narrow features in the LDOS of the sufficiently sharp Pt-coated tip apex lie below the mean Fermi level of metal electrodes, NDR should occur only at the negative tip bias.[30] This expectation is consistent with our experimental observation that no peak-shaped current dependence was observed in the positive bias region between 0 and +3 V.

The nature of charge transfer through the molecular states that leads to the observed NDR for the region of applied biases where narrow features in the LDOS of the tip apex couple with molecular levels can, in principle, be described by both one-step resonant tunneling[1−7] and two-step reduction/oxidation[8,31] processes. In the resonant tunneling mechanism, charge transfer results from the charge tunneling through appropriate molecular levels without occupying them.[4,32] The molecules themselves do not attain a charge over a time scale comparable to the phonon relaxation time. While this process can, in principle, describe the peak-shaped current observed here, it cannot adequately explain the origin of the peak in the bias-dependent redox adhesion force.

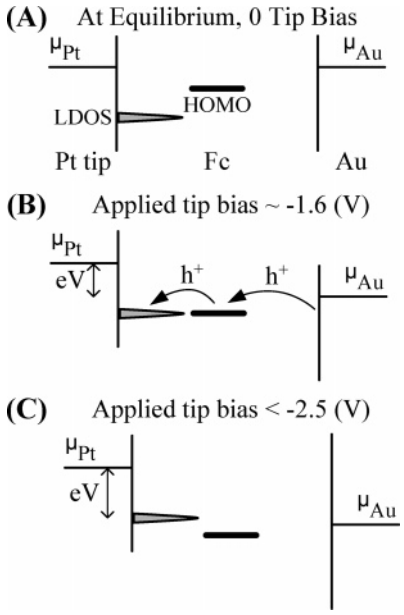

Figure 6. Schematic of how the LDOS of the tip apex could float relative to the HOMO of Fc under negative bias. (A) At equilibrium, $\mu_{tip} = \mu_{Au}$. (B) At a negative tip bias corresponding to the perfect alignment of the LDOS with the HOMO, hole transfer via sequential oxidation and subsequent reduction would lead to the maxima in both additional current and in the number of trapped positive charges. (C) At more negative tip biases, the LDOS would move away from alignment, leading to a decrease in current.

Unlike one-step charge transfer, in the reduction/oxidation mechanism, charge transfer occurs via sequential oxidation and subsequent reduction of electroactive terminal ferrocenes where charge is temporarily trapped by the phonon relaxation. Since the forces observed in the redox adhesion force versus bias dependence are attractive, ferrocene end groups are strong electron donors, and the LDOS of the tip apex lies below the mean Fermi level of metal electrodes, we argue that charge transfer primarily occurs through and in the HOMO of the Fc molecules. Though nonreversible change of the ferrocenylundecanethiol monolayer cannot be completely ruled out, we note that repeated measurements in the same area showed the same result on the second measurement, within experimental error.

The proposed mechanism for NDR and peak-shaped redox adhesion force based on the oxidation/reduction mechanism is shown schematically in Figure 6. The bias is applied to the tip, and the electrochemical potential of the gold substrate μ_{Au} is taken as energy reference. Figure 6A illustrates an equilibrium energy diagram with zero applied bias where the electrochemical potentials of the substrate and the tip are the same. The narrow features in the LDOS of the tip apex lie below the HOMO of Fc, and without alignment charge transport is primarily via nonresonant tunneling and no additional current is expected. As negative tip biases are applied, the LDOS sweeps closer to the HOMO level, and Figure 6B shows the relative energy levels under such negative tip bias when the narrow features in the LDOS of the tip apex align well with the HOMO of Fc, providing the largest coupling. Hole transfer is first from the gold substrate to the HOMO level of Fc, which oxidizes the molecule; the hole is temporarily trapped by the phonon relaxation of the molecular level to its new equilibrium

(28) Seminario, J. M.; De La Cruz, C. E.; Deroza, P. A. *J. Am. Chem. Soc.* **2001**, *123*, 5616.
(29) Snyder, S. R.; White, H. S. *J. Electroanal. Chem.* **2001**, *393*, 177.
(30) Xue, Y.; Datta, S.; Hong, S.; Reifenberger, R.; Henderson, J. I.; Kubiak, C. P. *Phys. Rev. B* **1999**, *59*, R7852.
(31) Mazur, U.; Hipps, K. W. *J. Phys. Chem.* **1995**, *99*, 6684.
(32) Schmickler, W. J. *J. Electroanal. Chem.* **1992**, *336*, 213.

configuration. A thermal fluctuation then allows subsequent hole tunneling from the molecular level of the molecule to the tip, returning the molecule to its neutral state. The largest coupling between the narrow features in the LDOS of the tip apex and the HOMO molecular level leads to the maxima both in additional current and in the number of trapped positive charges. In this configuration, the negatively charged tip provides a stabilizing electric field for the formation of ferricenium cations, similarly to counterions in an electrolyte solution. This is consistent with our observation that when the tip is removed from surface contact for ~5 s time delay between every measurement, no deviation from theoretical dependence was observed in the noncontact capacitive force for both tip bias polarities. This implies that the interface is not charged and that those cations are stable for less than several seconds. As more negative tip biases are applied, coupling between the narrow features in the LDOS of the tip apex and the HOMO molecular level decreases (see Figure 6C), moving the interface away from resonance and leading to a decrease in both current magnitude and number of cations and, hence, a decrease in the redox adhesion force. We next address the extent of interface charging.

Number of Trapped Charges Generated under the Negatively Biased Tip. The force-dependent number of molecules forming the junction can be estimated from the contact area using a Hertzian elastic contact model with the adhesion force between the probe and sample included.[33] The contact area, a^2, between a spherical tip of radius R penetrating into a uniform elastic film may be estimated as:

$$a^2 = \left(\frac{FR}{K}\right)^{2/3} \tag{5}$$

where F is the interaction force and K is an effective modulus equaling $(4/3)[(1 - \upsilon_t^2)/E_t + (1 - \upsilon_s^2)/E_s]^{-1}$ (E_s, υ_s, E_t, and υ_t are Young's modulus and Poisson's ratio of the sample and Pt-coated AFM tip, respectively). The Poisson ratio for most materials is between 0.25 and 0.5, and hence, assuming $\upsilon_t \approx \upsilon_s \approx 0.33$, an effective modulus can be approximated as $K = 1.5E_tE_s/(E_t + E_s)$. Although measured values for elasticity modulus are not available, assuming $E_t = 170$ GPa[34] and $E_s = 7$ GPa,[35] the contact area for the maximum applied interaction force of 20−30 nN would be 7.8−10.2 nm^2. The surface coverage for a closely packed $FcC_{11}SH$ SAM is about 2.5 molecules/nm;[2,36] thus, there are about 20−25 molecules in direct contact between the AFM tip and the substrate under 20−30 nN interaction force.

The deviation magnitude of 1.7 ± 0.4 nN observed in the bias-dependent adhesion force dependence may be used to estimate the total trapped charge Q. The additional attractive force arises from Coulombic interactions between the stored charge and its image charges in the tip and Au substrate. Using a simple parallel-plate geometry[37] and assuming that stored charge is localized on the ferricenium end groups, we find that the quantity of detected charges is $Q = 80 \pm 20$ positive elementary charges or the same number of oxidized molecules if we assume each molecule can store one charge. We note that the obtained number of charges is 3 to 4 times higher than the maximum number of molecules (20−25) in direct contact with the AFM tip. This is reasonable given that the field extends beyond the region of contact, which could enable the lateral migration of charges. It is also possible that the parameters used in the above model overestimate the amount of charge and/or underestimate the number of molecules. Since measured values for elasticity modulus are not available, if we were to consider $E_s = 1$ GPa instead of 7 GPa as used above, we would estimate that there are about 72−110 molecules in direct contact between the AFM tip and the substrate under 20−30 nN interaction force, reasonably close to ~80 positive elementary charges obtained above.

Conclusions

We have presented a method to measure charge within a molecular circuit that shows negative differential resistance via conducting probe atomic force microscopy. This has been facilitated by using a prototypical redox species, ferrocene, in a metal−molecule−metal junction. We observed that the voltage region over which conduction was enhanced correlated strongly with the region over which the scanning probe tip experienced capacitive attraction to the surface. A model for the capacitance force shows that the force originates primarily at the apex of the tip, and the bias dependence indicates that the trapped charges are holes. The number of charged ferrocenylundecanethiol molecules appears to exceed the number that is in direct mechanical contact with the tip when current flows.

Acknowledgment. We gratefully acknowledge financial support from the NSF (CHE-0404579), ARO (W911NF-04-100191), and the ONR (N00014-02-1-0327).

JA0514491

(33) Weihs, T. P.; Nawaz, Z.; Jarvis, S. P.; Pethica, J. B. *Appl. Phys. Lett.* **1991**, *59*, 3536.
(34) Burnham, N, A.; Colton, R. J. *J. Vac. Sci. Technol., A* **1989**, *7*, 2906.
(35) Joyce, A.; Thomas, R. C.; Houston, J. E.; Michalske, T. A.; Crooks, R. M. *Phys. Rev. Lett.* **1992**, *68*, 2790.
(36) Chidsey, C. E. D.; Bertozzi, C. R.; Putvinski, T. M.; Mujsce, A. M. *J. Am. Chem. Soc.* **1990**, *112*, 4301.
(37) Schaadt, D. M.; Yu, E. T.; Sankar, S.; Berkowitz, A. E. *Appl. Phys. Lett.* **1999**, *74*, 472.